Journal of the Ceramic Society of Japan 117 [9] 987-991 2009 Paper

Effect of mixing condition of additives on the solidification of green body by gelcasting method

Tomoaki KATO, Takashi SHIRAI, Hideo WATANABE, Masayoshi FUJI,† Minoru TAKAHASHI, Yusuke YAMADA,* Shuichi IWATA,* Yoshihito KATO* and Hideki MORI*

Ceramics Research Laboratory, Nagoya Institute of Technology, 3–101–1, Honmachi, Tajimi, Gifu 507–0033
***Department of Material Engineering, Nagoya Institute of Technology, Gokiso, Showa, Nagoya, Aichi 466–8555**

In order to find out conditions for fabricating green body with no defect in gelcasting method, effect of mixing conditions of additives on solidification process of ceramics slurry has been examined in this study. Flow pattern of alumina slurry is deduced by considering actual power consumption of an agitation mixer as well as Reynolds number of agitation calculated, and then compared with observation of solidified green body. The effects of mixing condition is described as a function of the rotation speed and related to flow regimes such as laminar, transition and turbulent flow. It has been found that the boundary between the transition and turbulent flow region is the most suitable for gelcasting method.

Key-words : Gelcasting, Mixing condition, Power consumption, Green body

[Received May 12, 2009; Accepted August 20, 2009]

1. Introduction

Gelcasting method[1),2)] is stable for fabricating complex-shaped green body with a high uniformity of particle-packing structure.[3)] In this method, ceramics slurry including gelants such as monomer and closs-linker is solidified by gelation reaction, which is usually radical polymerization of organic monomer. To initiate and facitate the polymerization, additives such as initiator and catalyst are added into the slurry. Requirements for realizing a good quality and uniformity of green body in this method are preparation of stable and high solid-loaded slurry and homogeneous gelation. There are a number of literatures for the preparation of well-dispersed slurry[4)–7)] and the solidification process.[8)–10)] The latter mainly focused on optimization in the amount of the additives to loading of monomer and solids. Well mixing of the additives into the slurry should be addressed as another important aspect in the solidification process. If non-uniform concentration of additives was caused by poor-mixing, the gelation and resultant gel structure could not be homogeneous. The non-uniform gel structure may cause problems such as fracture, warp and clack propagation in processes of drying, debindering and sintering. Therefore, it is important to consider mixing conditions of the additives in order to fabricate uniform-structured green body in the gelcasting method.

In this study, a comparison of flow pattern in the slurry and state of gel-green body has been conducted to understand the effect of mixing condition. At first, flow pattern of alumina slurry in an agitation vessel with an impeller was estimated by Reynolds number of agitation and power number. To evaluate these numbers, torque of a shaft in the agitation vessel at various rotational speeds of the impeller is measured. Secondly, gel state of green body is compared with the flow pattern to find out the suitable mixing condition. The slurry is solidified by adding of initiator and catalysis under mixing in the vessel at each rotational speed and then the solidified body is cut to be observed for its cross section. The suitable mixing condition will be described as a function of the rotation speed and related to flow regimes such as laminar, transition and turbulent flow.

2. Experimental procedure

2.1 Preparation of slurry

Table 1 shows the composition of slurry used in this study. Grade AL 160 SG–4 alumina powder (Showa Denko Co., Yokohama, Japan) was used. The mean particle size was 0.5 μm. The dispersant used was an ammonium salt of polycarboxylate (Seruna D–305, Chukyo Yushi, Nagoya, Japan). Methacrylamide and N,N'-methylene-bis-acrylamide were used as an organic monomer and a cross-linker, respectively. Distilled water was used for solvent. The initial slurry was prepared by ball-milling for 24 h. The slurry was agitated and degassed under a vacuum condition for 15 min..

2.2 Measurement of rheological properties

The rotational flow between parallel disks (H_r = 1 mm, φ = 60 mm) of Rheostress 600 system (Haake GmbH, Germany) was used for measurements of rheological property of the slurries.

2.3 Measurement of power consumption

The torque of the shaft in the agitation vessel was measured by two types of torque meter. HEIDON–BL1200Te (Shinto

Table 1. Composition of Slurry

	mass%
alumina	80.1
distilled water	15.1
dispersant	0.7
monomer	3.2
closs-llinker	1.1

† Corresponding author: M. Fuji; E-mail: fuji@nitech.ac.jp

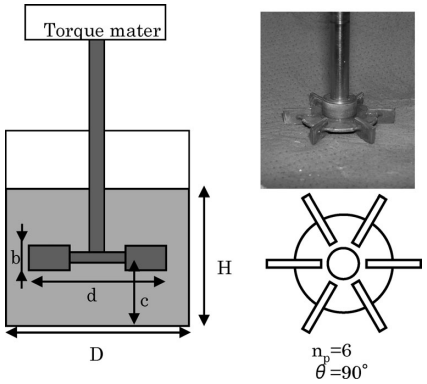

Fig. 1. Schematic drawings of the apparatus and photograph of the disk turbine impeller.

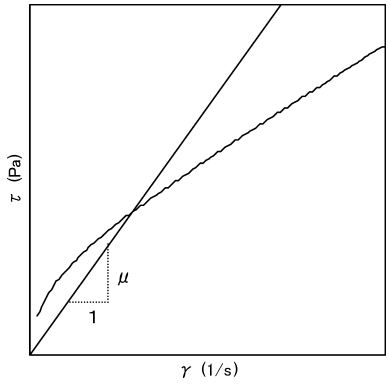

Fig. 2. Slope fitting image for Metzner-Otto method.

Table 2. Size of Vessel and Impeller Diameters

impeller	small	midlle	large
d (mm)	50	75	100
D (mm)	85	125	170
H (mm)	63	95	126
b (mm)	10	15	20

Table 3. Power Correlation for a Paddle Impeller

Power consumption: P (Power number: $Np_{exp} = P/(\rho N^3 d^5)$)
$Np_{cal} = \{[1.2\pi^4\beta^2]/[8d^3/D^2H]\}f$
$f = C_L/\mathrm{Re}_G + C_t\{[(C_{tr}/\mathrm{Re}_G) + \mathrm{Re}_G]^{-1} + (f_\infty/C_t)^{1/m}\}^m$
$\mathrm{Re}_d = Nd^2\rho/\mu$ (impeller Reynolds number)
$\mathrm{Re}_G = \{[\pi\eta \ln(D/d)]/(4d/\beta D)\}\mathrm{Re}_d$
$C_L = \{0.215\eta n_p(d/H)[1-(d/D)^2] + 1.83\,(b/H)(n_p/2)^{1/3}\}$
$C_t = \{[1.96X^{1.19}]^{-7.8} + (0.25)^{-0.78}\}^{-1/7.8}$
$m = [(0.71X^{0.373})^{-7.8} + (0.333)^{-0.78}]^{-1/7.8}$
$C_{tr} = 23.8(d/D)^{-3.24}(b/D)^{-1.18}X^{-0.74}$
$f_\infty = 0.0151(d/D)C_t^{0.308}$
$X = \gamma n_p^{0.7} b/H$
$\beta = 2\ln(D/d)/[(D/d) - (d/D)]$
$\gamma = [\eta \ln(D/d)/(\beta D/d)^5]^{1/3}$
$\eta = 0.711\{0.157 + [n_p \ln(D/d)]^{0.611}\}/\{n_p^{0.52}[1-(d/D)^2]\}$

Scientific Co., Tokyo, Japan) was used for the biggest vessel and impeller, and ST–1000 (Satake Chemical Equipment Mfg Ltd., Tokyo, Japan) was used for the other case.

Figure 1 shows a schematic diagram of the experimental apparatus and photograph of the disk turbine impeller (d = 50 mm), and its geometry. Three sets of the agitation vessel and impeller were prepared for the experiments. One of the experimental apparatus consisted of transparent cylindrical glass vessel (e.g., D = 85 mm and H = 63 mm for the smallest case) without baffles. The vessels were filled with the slurry. A disk turbine impeller (e.g., d = 50 mm, b = 10 mm for the smallest case) consisting of six blades was installed at the center of the vessel (c/H = 0.5). The size of vessels and impeller diameters used in the experiments are summarized in **Table 2**. The rotational speed N was varied from 50 rpm to 500 rpm.

2.4 Power consumption in a vessel without baffle

Here is briefly described estimation procedures of the observed power number, Np_{exp}, and the calculated power number, Np_{cal}, as well as the impeller Reynolds number, Re_d. The power consumption P is given from the measurements of the shaft torque T and the rotational speed N, as:

$$P = 2\pi NT \ . \tag{1}$$

The experimental power number (Np_{exp}) is defined as,

$$Np_{exp} = P/(\rho N^3 d^5) \ , \tag{2}$$

where ρ is a slurry density and d is the impeller diameter.

The impeller Reynolds number is defined as:

$$\mathrm{Re}_d = Nd^2\rho/\mu \ , \tag{3}$$

where μ is the slurry viscosity.

The calculated power number (Np_{cal}) can be estimated from Kamei's Eqs. (4) and (5),[11–13]

$$Np_{cal} = \left\{\left[1.2\pi^4\beta^2\right]/\left[8d^3/D^2H\right]\right\}f \ , \tag{4}$$

where D is the diameter of the vessel, H is liquid height in the vessel.

f is friction factor, defined as:

$$f = C_L/\mathrm{Re}_G + C_t\left\{\left[(C_{tr}/\mathrm{Re}_G) + \mathrm{Re}_G\right]^{-1} + (f_\infty/C_t)^{1/m}\right\}^m \ , \tag{5}$$

where the first term of the right hand side contributes in the laminar flow region and second one in the turbulent flow region. Correlation factors in Eqs. (4) and (5) are summarized in **Table 3**, where b and n_p are paddle width and the number of blade, respectively.

The rheological data, consistsing of shear rate $\dot{\gamma}$ versus the shear stress τ for the slurry measured by the rheometer, can give an apparent slurry viscosity (μ) at each shear rate. Following the Metzner-Otto method,[14] the shear rate can be calculated from a linear correlation between the rotational speed N and the shear stress as $\dot{\gamma} = k_s N$. Here, the Metzner-Otto constant was determined experimentally as k_s = 42.5 for the slurry.

2.5 Observation of green body

The green body was fabricated by adding of an initiator and a catalysis into the slurry under mixing in each rotational speed. Smallest impeller (φ50) was used for the mixing. The rotational speed was 100, 150, 200, 250, 300 or 500 rpm. Ammonium persulfate and N,N,N',N'-tetramethyletylenediamine were used as

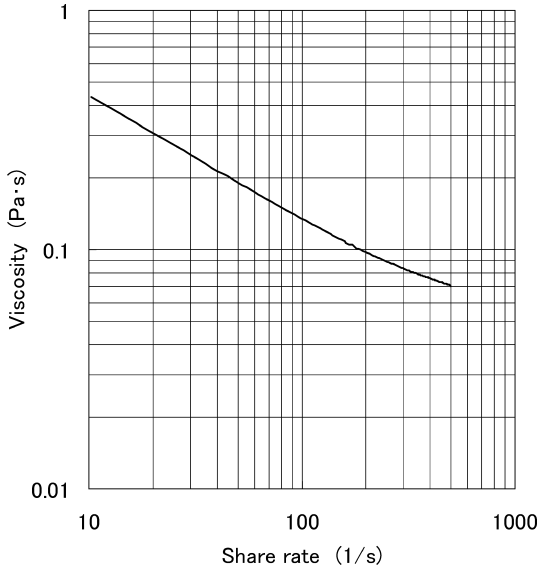

Fig. 3. Rheological property of slurry.

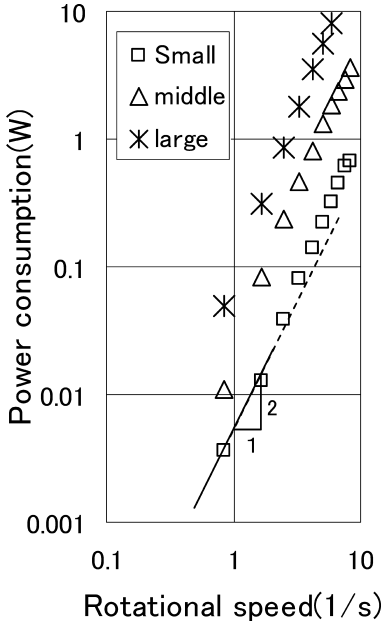

Fig. 4. Dpendence of power consumption on rotational speed.

the initiator and the catalyst, respectively. The 926 μl of the initiator (10 wt% aqueous solution) was added into 900 g of the slurry in the vessel under mixing for 3 min., followed by adding 262 μl of the catalyst and mixing for 3 min. The impeller was stopped rotating and left for 30 min. And then was pulled out from the slurry. The slurry was left in the vessel for another 30 min. and then the solidified body was removed from vessel and cut to be observed for its cross section.

3. Results and discussion

3.1 Relationship between Reynolds number of agitation and power number

Figure 3 shows the viscosity of the alumina slurry as a function of share rate. The viscosity decreases with increasing of share rate. In the mixing vessel, there is a distribution of share rate and viscosity. Characteristic share rate was determined by Metzner-Otto method for each rotational speed. The characteristic viscosity was estimated by the Fig. 3 for each characteristic share rate and used for Eqs. (2) and (3) to calculate Reynolds number of agitation and power number.

Boundaries of flow states were estimated by relationship between rotational speed of impellers and power consumption calculated from the torque of the impeller shaft using Eq. (1) as shown in **Fig. 4**. The boundary between laminar flow and transition region can be deduced by fitting data with the logarithmic line with slope of 2 in this figure.[12] In this case, region from 1.67 to 2.5 s^{-1} (100–150 rpm) for the small impeller is fit with the slope of 2. The Reynolds number of agitation on 2.5 S^{-1} (150 rpm) with small impeller was 76. This is the boundary value of the laminar flow. The boundary of turbulent flow region could be confirmed by air entrainment into the slurry under the mixing. At 300 rpm, small babbles by the air entrainment were confirmed on the slurry surface and it is thought that the Reynolds number of agitation at the boundary of transfer region and turbulent region is 400.

Figure 5 shows the relationship between Reynolds number of agitation and power number. The measured values of power number are in good agreement with the calculated values. It has been verified that the calculation procedure described in the section 2.2 in this paper is pretty reasonable to estimate the mixing

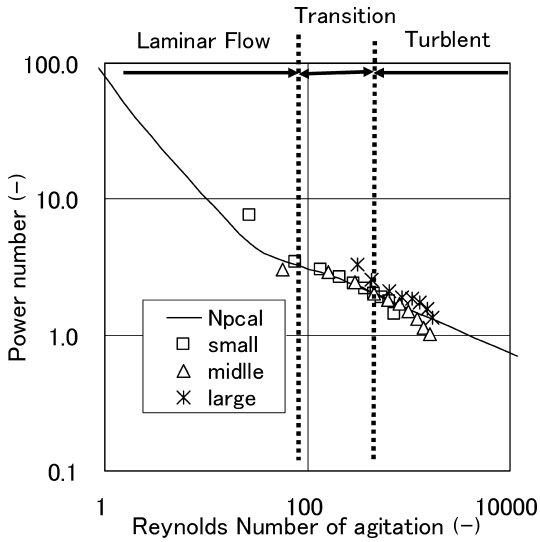

Fig. 5. Power consumption of slurry mixing with calculated walue.

condition of the slurry. The boundaries between flow states determined by the results of Fig. 4 are shown in this figure. The turbulent flow was occurs easily by increasing of the paddle size. And, it was able to be confirmed that each flow states were well reproduced by the small paddle.

3.2 Observation of green body

Figure 6 shows cross-section photos of green bodies prepared with different rotational speeds and gelling times, which are defined as elapsed time since the rotation of the impeller has been stopped (see section 2.5). At 100 rpm, the gel body for gelling time of 60 min. is too soft to keep its shape. At 150 and 200 rpm for 60 min., strength of gel is enough to keep the shape of green body. In these conditions corresponding laminar flow, the gel bodies are non-uniform and have holes, which correspond to donuts-ring like area not gelled after 60 min. Over 250 rpm, the

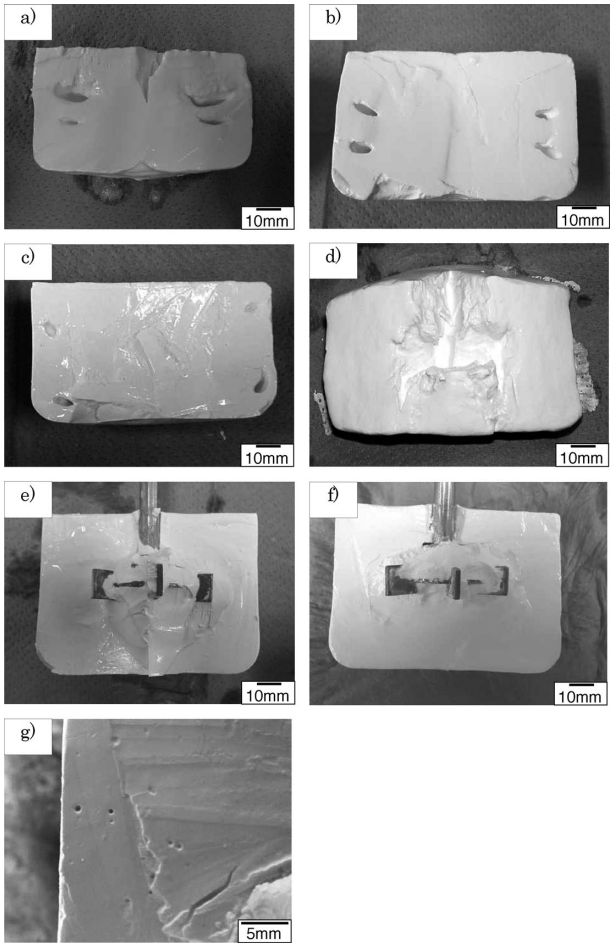

Fig. 6. Cross-section photo of green bodies prepared with different rotational speed : (a) 100 rpm, (b) 150 rpm, (c) 200 rpm, (d) 250 rpm, (e) 300 rpm, (f) 500 rpm and (g) small holes at 500rpm.

slurry can be solidified for 30 min. which is shorter than previous. At 250 rpm, the gel is uniform but not so strong that deformation can be seen in the photo. At 500 rpm, the body is fairly hard but many small holes are seen, which are originated from bubbles entrained by mixing with turbulent flow region. In the range of this study, 300 rpm is the best condition of mixing in gelcasting which corresponds to boundary between transition and turbulent flow regions.

Figure 7 shows schematic illustrations of flow patterns for each flow regime. In laminar flow region (Fig. 7(a)), the flow is so stable that the additives added can not be uniformly distributed in the slurry. Unmixed areas as shown in this figure correspond to the doughnuts-rings as shown in Fig. 6 at 100–200 rpm. Turbulent flow (Fig. 7(c)) produces obviously wall-mixing so that the additives can be distributed uniformly. However, bubbles were entrained from regions around the impeller shaft, and became small holes in solidified body. In transition flow region (Fig. 7(b)) the flow is not stable and changes rapidly between laminar-like and turbulent-like. This can produse well-mixing of additives but no bubble entrainment. In summary, it has been segedted that transition flow region is the best condition in gelcasting for fabricating gel-green bpdywoth uniform structure and no defect (babble-holes).

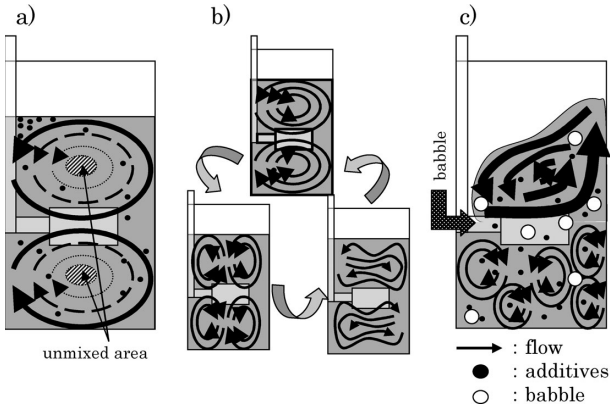

Fig. 7. Flow pattern model in each region: (a) Laminar flow, (b)Transition, (c)Turbulent flow.

4. Conclusions

In order to find out conditions for fabricating green body with no defect in gelcasting method, effect of mixing conditions of additives on solidification process of slurry has been examined in this study. Follow pattern of alumina slurry was deduced by considering actual power consumption of an agitate mixer as well as Reynolds number of agitation calculated. The measured values of power number were in good agreement with the calculated values, so that the calculation procedure was verified to be reasonable to estimate the mixing condition of the ceramic slurry. The flow pattern was compared with state of solidified green body. Lower rotational speed resulted in a weak gel body and doughnuts-ring like not geled, which corresponded to laminar flow regions. Higher rotational speeds corresponding to transition regions gives uniformed green body with no hole, but excessive higher speed corresponding to turbulent flow regions caused small holes in the green body originated from bubbles entrained in the slurry by mixing. The results have revealed the importance in mixing conditions of additives in the slurry for gelcasting method.

Acknowledgement This research was carried out by the Ministry of Education, Culture, Sports, Science, and Technology (MEXT) financed project “Cooperation for Innovation Technology and Advanced Research in Evolution Area”.

Nomenclature

T = Torque [Nm]
P = power consumption [W]
N = Impeller rotation speed [1/s]
ρ = slurry density [kg/m^3]
d = impeller diameter [m]
μ = slurry viscosity [Pas]
D = vessel diameter [m]
H = slurry height [m]
b = paddle width [m]
n_p = number of blade [–]
$\dot{\gamma}$ = shear rate [1/s]
τ = shear stress [Pa]

References

1) O. O. Omatete, M. A. Janney and R. A. Strehlow, *Am. Ceram. Soc. Bull.*, 70[10], 1641–1649 (1991).
2) A. C. Young, O. O. Omatete and M. A. Janney, *J. Am. Ceram. Soc.*, 74[3], 612–618 (1991).
3) M. A. Janney, W. Ren, G. H. Kirby, S. D. Nunn and S. Viswanathan, *Mater. Manuf. Process*, 13[3], 389–403 (1998).
4) J. Tong and D. Chen, *Ceram. Int.*, 30[8], (2004) 2061–2066
5) F. Valdivieso, P. Goeuriot and F. Thevenot, *J. Eur. Ceram. Soc.*, 17[2], 377–382 (1997).
6) C. Takai, M. Tsukamoto, M. Fuji and M. Takahashi, *J. Alloys Compd.*, Vol. 408–412, 533–537 (2006).
7) B. P. Singh, R. Menchavez, M. Fuji and M. Takahashi, *J. Colloid Interface Sci.*, 300[1], 163–168 (2006).
8) M. Potoczek and E. Zawadzak, *Ceram. Int.*, 30[5], 793–799 (2004).
9) A. A. Babaluo, M. Kokabi and A. Barati, *J. Eur. Ceram. Soc.*, 24[4], 635–644 (2004).
10) M. Kokabi, A. A. Babaluo and A. Barati, *J. Eur. Ceram. Soc.*, 26[15], 3083–3090 (2006).
11) N. Kamei, S. Hiraoka, Y. Kato, Y. Tada, S. Kuwabara, Y. S. Lee, T. Yamaguchi and S.-T. Koh, *Kagaku Kogaku Ronbun*, 20, 595–603 (1994).
12) S. Hiraoka, Y. Kato, Y. Tada, N. Ozaki, Y. Murakami and Y. S. Lee, *Trans. IChemE*, 79, Part A, 805–810 (2001).
13) S. Hiraoka, Y. Tada, Y. Kato, A. Matsuura, T. Yamaguchi and Y. S. Lee, *J. Chem. Eng. Jpn.*, 34, 1499–1505 (2001).
14) A. B. Metzner, R. H. Feehs, H. L. Ramos, R. E. Otto and J. D. Tuthill, *AIChE J*, 7, 3–9 (1961).